Study of the Feasibility of an EEDF Driven Rare Gas Metastable Laser

Guy Parsey[A], Yaman Güçlü[B], John Verboncoeur[A], Andrew Christlieb[A]

[A]Michigan State University, [B]Max-Planck Institute

Supported by AFOSR and a MSU Stategic Partnership Grant

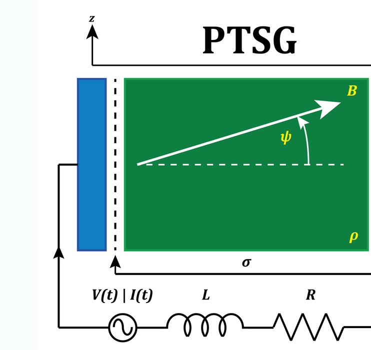

Abstract

Motivation for the rare gas laser (RGL) was instigated by a similarity between the excited level structures of alkali metals used in a diode-pumped alkali laser (DPAL) and those of metastable excitations of noble gas species. First presented experimentally by Han and Heaven, the spectral properties are extremely similar between the DPAL and RGL pumping transition.[1] However, rare gas metastables have the benefit of being chemically inert and gaseous without heating. The RGL use an electric discharge to maintain the metastable species densities, analogous to heating for the alkali vapor, while both focus on optical pumping to induce lasing with a three-level scheme. We propose using a modified electron energy distribution function (EEDF) to either modify RGL efficiency characteristics or to drive the optical gain process.

Using our general-purpose kinetic global modeling framework (KGMf), we present a study on the effect of the EEDF on the Argon RGL reaction kinetics with an emphasis on determining if lasing can be achieved without optical pumping. We first model the optically driven system to create a gain efficiency baseline and verify the implemented intensity driven laser model against the simulation work presented by Demyanov et. al.[2] With a comparative baseline, we then look at the effectiveness of using a microwave induced EEDF to either modify optical driven RGL characteristics or maintain the lasing state population inversion without a driving laser.

DPAL to RGL

DPAL, first published by Krupke et. al. [2], demonstrating three-level laser oscillation between the $^2S_{1/2}$, $^2P_{1/2}$, and $^2P_{3/2}$ excited levels of Rb.

+ Wide-band incoherent pumping to drive
- Requires vaporized alkali metal

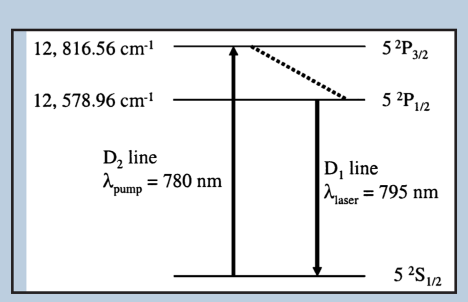

Spectral properties similar to transitions between the noble gas excitations $(n+1)s[3/2]_2$, $(n+1)p[1/2]_1$,and $(n+1)p[5/2]_3$ [3]. Uses

- Inert reagent operating at room temperature
- Collision partners to relax upper level
- Pumping transition probabilities, upper state radiative lifetimes, lasing wavelengths and pressure broadening coefficients analogous to DPAL

In both traditional cases, incoherent pumping is used to drive the laser oscillation.

Kinetic Global Modeling Framework

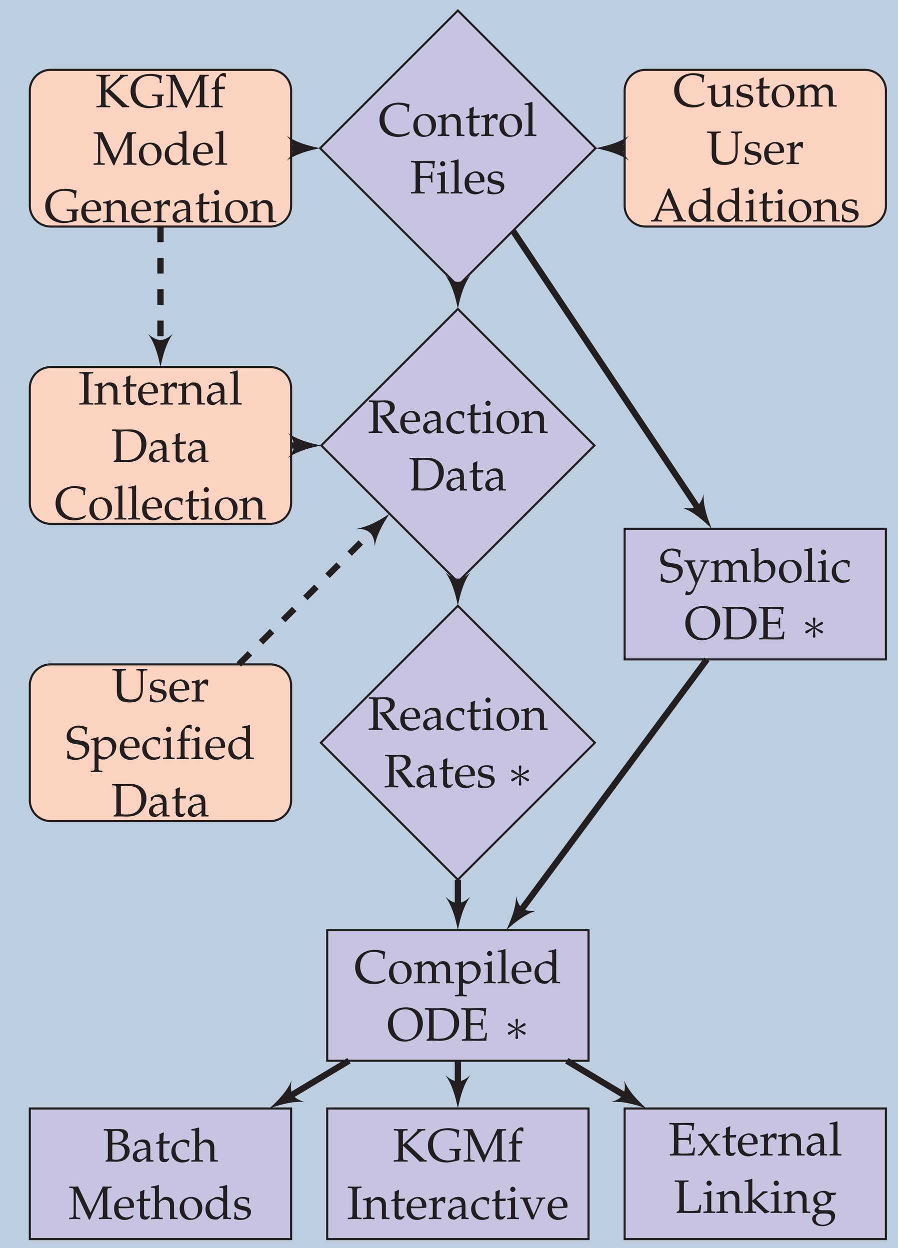

Two control files define the reaction network ODE model

Reaction File

- Reaction pathways and ODE species
- Mapped reactions ref. from KGMf database
- User specified states, reactions, or alternate reaction data

Simulation File

- Non-species (e.g. T_e) derivative equations
- *dim*(ODE model)
- EEDF specification
- System parameters (e.g. abs power)

Readability, manipulation, and recoverability (∗) emphasized

- Symbolic ODE dependent only on reaction pathways
- Reaction terms: wrapped symbolically
  - Analytic expressions of ODE and system variables
  - Shared-knot spline vectorization
  - Python-wrapped integrations with ODE variables
- Jacobian found symbolically with modified rates
- Compiled to C code with common subexpression simplification

Standard KGM

General species continuity and effective electron energy equation (solved for T_e)

$$\frac{dn_\alpha}{dt} = \sum_i^R \nu_i^\alpha K_i \prod_j n_j - \frac{D_{\text{eff}}}{\Lambda^2}$$

$$\frac{d}{dt}\left[\frac{3}{2}n_e T_e\right] = \frac{P_{\text{eff}}}{V} - n_e \sum_i^{R_{\text{EI}}} n_i K_{ij} \Delta E_{ij}$$

- P_{eff} for RF and MW sources
- e^--impact reaction rates depend on EEDF
  - Electronic and ionization excitation
- Includes spontaneous emission w/o tracking spectral density

$$K_i(x,\vec{a}) = \int_0^\infty d\varepsilon\, v(\varepsilon)\sigma_i(\varepsilon) f_e(\varepsilon,\vec{a})$$

EEDF can be defined numerically (2D including ε) or algebraically (arbitrary number of parameters)

- Known physically allowed algebraic forms
- BOLSIG+ calculated EEDF vs T_e or ion frac

Example normalized parameterized EEDF

$$f_e = \frac{x\varepsilon^{\frac{1}{2}}}{(\frac{3}{2}T_e)^{\frac{3}{2}}} \frac{(\Gamma(\frac{5}{2x}))^{\frac{3}{2}}}{(\Gamma(\frac{3}{2x}))^{\frac{5}{2}}} \exp\left[-\left(\frac{\Gamma(\frac{5}{2x})}{\Gamma(\frac{3}{2x})}\frac{\varepsilon}{\frac{3}{2}T_e}\right)^x\right]$$

Laser Modeling

Joining the species equations is the continuity equations for the average two-way laser intensity [1]

$$\frac{d\Psi(t)}{dt} = (t_{\text{L}} R e^{2l_g\beta_{21}} - 1)\frac{\Psi}{\tau_{\text{rt}}} + n_2\frac{\sigma_{21}c^2 h\nu_{21}}{l_g}$$

where n_2 and n_1 are the number density of the lasing and lower level species, σ_{21} is the stimulated emission cross section, and the stimulated emission and β, the weigthed population inversion, terms are

$$\tilde{K}_{ij}^{\text{stim}} = \beta_{ij}\frac{\Psi}{h\nu_{ij}} \quad \text{and} \quad \beta_{21} = \sigma_{21}(n_2 - \frac{g_2}{g_1}n_1)$$

Output laser intensity is found as a post-processing artifact of the two-way laser intensity with an experimental tuning parameter η

$$I_{\text{Lase}}(t) = \eta\Psi(t)\frac{l_g\beta t_{\text{L}}(1-R)e^{l_g\beta}}{(e^{l_g\beta}-1)(1+t_{\text{L}}^2 R e^{l_g\beta})}$$

Optical pumping of a specific transtion, ν_{kl}, can be treated as a reaction term $\tilde{K} = \Omega_{kl}/h\nu_{kl}$, where α is defined as β and the absorbed power per unit volume

$$\Omega(t) = \frac{P_P(t)}{l_g} t_P(1-e^{l_g\alpha_{kl}})(1+t_P^2 R_P e^{l_g\alpha_{kl}})$$

Where P_P is a (repeated) gaussian time pulse

EEDF Driven RGL

Using the pure Argon case as an example peice

- Full model with all $4s$ and $4p$ states
- Toy model with ground and laser levels

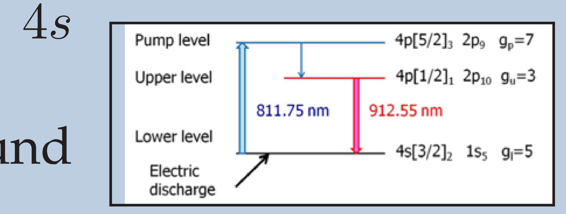

Using the full model, first look at capability of MW to drive population inversion with EEDF selection

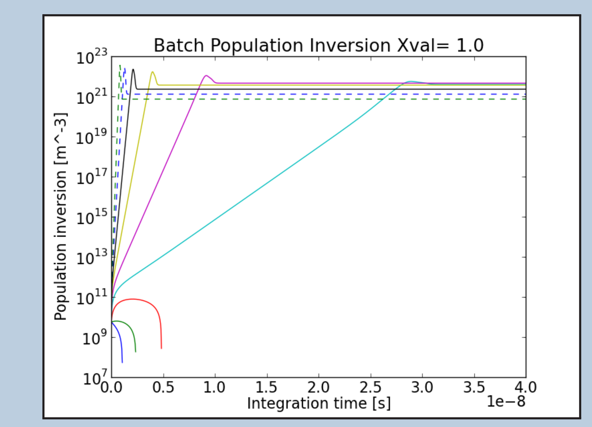

Parameterization
$X = 1 \Rightarrow$ Maxwellian
$X = 2 \Rightarrow$ Druyvesteyn

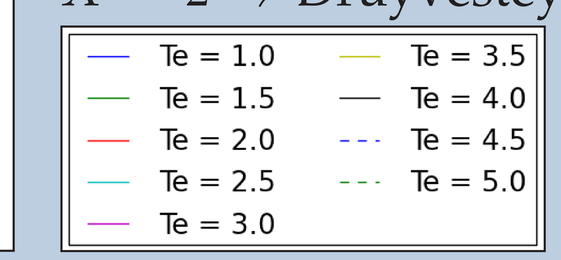

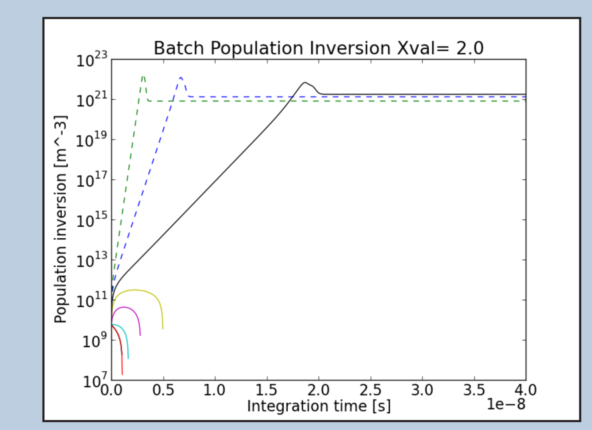

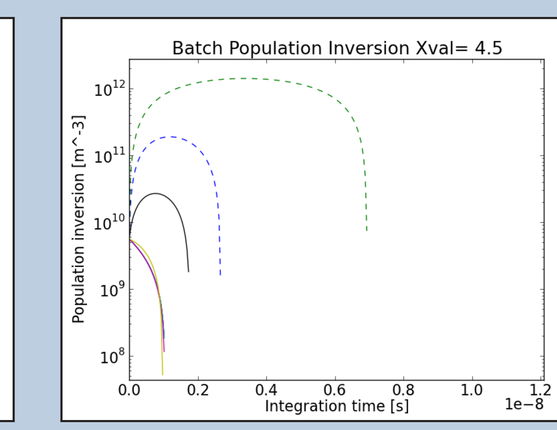

Recreating the optically pumped model presented by Demyanov et. al. [1], we compare the bahavior of the toy (left) to the complete argon model (right).

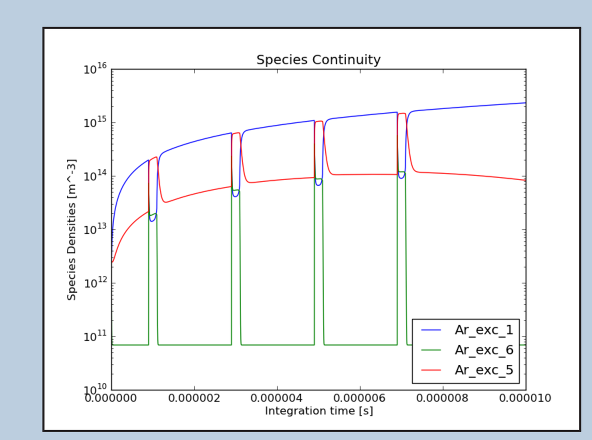

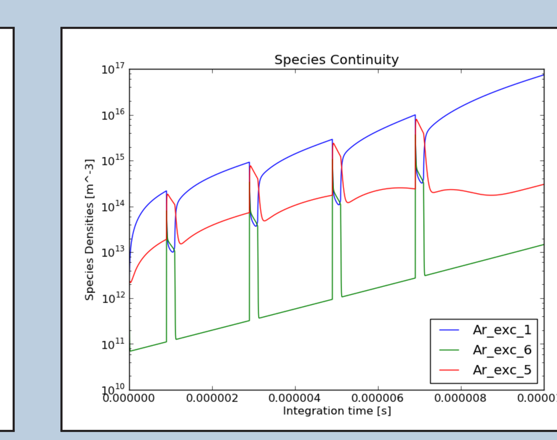

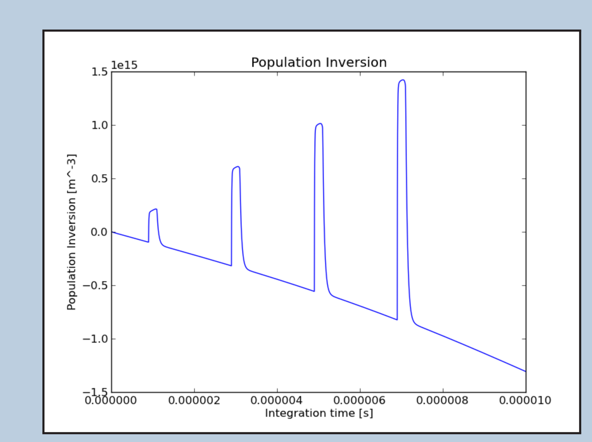

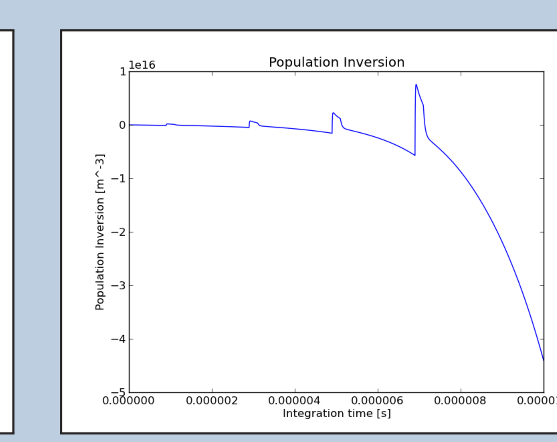

Only those states shared by the toy model are plotted for comparison. The trending differences show that the toy model is only applicable for testing.

References

[1] I. V. Kocketov A. V. Demyanov and P. A. Mikheyev. *J. Phys. D*, 46:375202–10, July 2013.

[2] V. K. Kanz W. F. Krupke, R. J. Beach and S. A. Payne. *Opt. Lett.*, 28(23):2336–38, Dec 2003.

[3] J. Han and M. C. Heaven. *Opt. Lett.*, 37(11):2157–59, June 2012.